

Reproduced by permission of Kluwer Academic Publishers, Dordrecht, Boston, London

---

Space Science Reviews 60: 565-590, 1992. © 1992 Kluwer Academic Publishers. Printed in Belgium.

---

## GALILEO RADIO SCIENCE INVESTIGATIONS

H. T. HOWARD, V. R. ESHLEMAN, D. P. HINSON

Center for Radar Astronomy, Stanford University, Stanford, CA 94305. U.S.A.

A. J. KLIORE, G. F. LINDAL, R. WOO

Jet Propulsion Laboratory, U.S.A.

M. K. BIRD, H. VOLLAND

Radioastronomisches Institut, Universität Bonn. Germany

P. EDENHOFER

Institut für HF-Technik, Universität Bochum. Germany

M. PÄTZOLD and H. PORSCHE

Deutsche Forschungsanstalt für Luft- und Raumfahrt, Germany

---

**Abstract.** The radio science investigations planned for Galileo's 6-year flight to and 2-year orbit of Jupiter use as their instrument the dual-frequency radio system on the spacecraft operating in conjunction with various US and German tracking stations on Earth. The planned radio propagation experiments are based on measurements of absolute and differential propagation time delay, differential phase delay, Doppler shift, signal strength, and polarization. These measurements will be used to study: the atmospheric and ionospheric structure, constituents, and dynamics of Jupiter; the magnetic field of Jupiter; the diameter of Io, its ionospheric structure, and the distribution of plasma in the Io torus; the diameters of the other Galilean satellites, certain properties of their surfaces, and possibly their atmospheres and ionospheres; and the plasma dynamics and magnetic field of the solar corona. The spacecraft system used for these investigations is based on Voyager heritage but with several important additions and modifications that provide linear rather than circular polarization on the *S*-band downlink signal, the capability to receive *X*-band uplink signals, and a differential downlink ranging mode. Collaboration between the investigators and the spacecraft communications engineers has resulted in the first highly-stable, dual-frequency, spacecraft radio system suitable for simultaneous measurements of all the parameters normally attributed to radio waves.

# 1. Introduction

Galileo radio science comprises two main areas of investigation, each with its own experiment team. The radio propagation team, with members from Stanford, JPL, Bonn, Bochum, and DLR, has responsibility for investigations of the solar corona and a variety of aspects of the Jovian system. The celestial mechanics team, with members from JPL, will search for gravitational waves, conduct other experimental tests of general relativity, and investigate the gravitational fields of Jupiter and its satellites. The members of the propagation team, selected by NASA and BMFT/DLR\*, and their associates are the authors of this article. The celestial mechanics investigations are described in a companion paper (Anderson *et al.*, 1992).

The radio science investigations employ telecommunications equipment onboard the Galileo spacecraft along with a network of tracking stations on Earth operated by the United States and Germany. One of the important preflight functions of the two radio science teams has been to use scientific experience gained from previous missions to influence the design of the relevant instrumentation. As will be seen in this paper, what has resulted from this collaboration with the Galileo project is a highly capable radio science system.

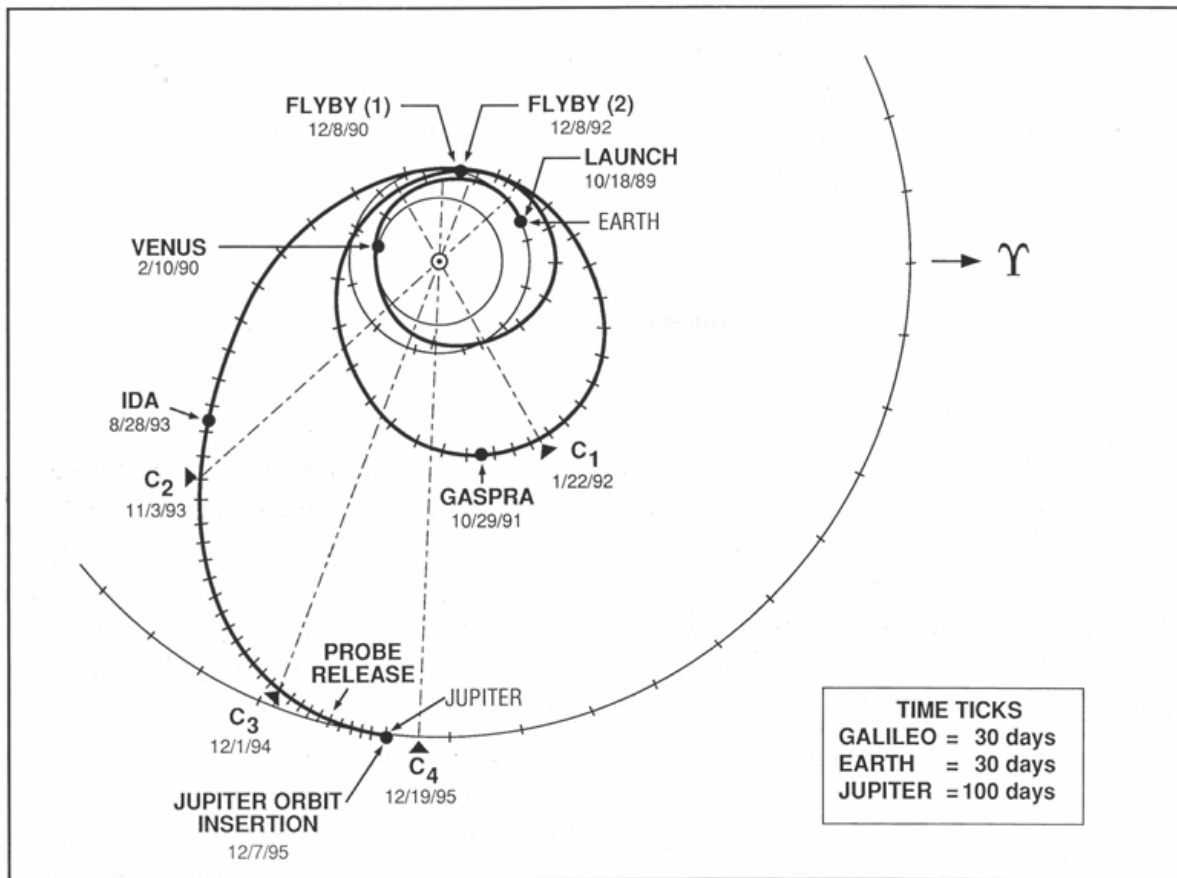


Fig. 1. Trajectory of the Galileo spacecraft (bold line) during its 6-year flight to Jupiter. The orbits of Venus, Earth, and Jupiter are also shown. Targets of opportunity for investigations

during this 'cruise phase' of the mission include Venus, Earth, and the asteroids Gaspra and Ida. The trajectory also provides observing geometries favorable to a search for gravitational waves; the best opportunities occur near solar opposition where the influence of the solar wind on the radio link with the spacecraft is at a minimum. Conversely, remote sensing of the solar corona will be conducted during solar conjunctions when radio signals propagating between spacecraft and Earth pass near the Sun. Three conjunctions occur during cruise and one follows shortly after orbit insertion at Jupiter; the spacecraft positions for these events are labeled C1, C2, C3, and C4.

Figure 1 shows the trajectory of Galileo during its 6-year flight to Jupiter, which includes geometries favorable to several radio science investigations. Of interest here are the solar conjunctions during which radio signals propagating between spacecraft and Earth pass near the Sun, providing an opportunity for remote sensing of the structure and dynamics of the solar corona. After arriving at Jupiter, the spacecraft will execute a 2-year nominal mission comprising ten to eleven orbits of the planet. This tour of the Jovian system will include repeated occultations of the spacecraft by Jupiter as well as occultations by and close encounters with each of the Galilean satellites. Radio occultation and bi-static radar measurements during these events will extend our understanding in diverse areas ranging from atmospheric dynamics on Jupiter to the properties of the surfaces of the icy Galilean satellites.

This paper is organized as follows. The next section describes the instrumentation and some of the basic measurement techniques used in radio science experiments. Subsequent sections describe the various radio propagation investigations roughly in their order of occurrence in the mission: the solar corona, atmospheres and ionospheres in the Jovian system, and the surfaces of the icy Galilean moons. Readers who are interested primarily in anticipated results can skip directly to the later sections; we have attempted to write these so that each can be read and understood independent of all others.

## 2. Radio Science Instrumentation and Measurement Techniques

### 2.1. INSTRUMENTATION

The telecommunications equipment on Galileo closely resembles that of the Voyager spacecraft (Eshleman *et al.*, 1977; Tyler, 1987). The basic system includes the capability to transmit two radio signals at coherently-related frequencies of about 8400 MHz (*X*-band) and 2300 MHz (*S*-band). The exact frequencies of the downlink signals depend on the operating mode of the spacecraft equipment but are always in the ratio of 11/3. The two signals are radiated through the main spacecraft antenna, a 4.8-m paraboloid attached to the spinning portion of the spacecraft and aligned with the axis of rotation. Table I summarizes key characteristics of the Galileo spacecraft radio system.

Two operating modes, selectable by commands sent to the spacecraft, are used in radio science experiments. In the 2-way coherent mode, used, for example, in tracking the motion of the spacecraft, the downlink frequencies are controlled by the coherent turnaround of an uplink signal received at either *S*- or *X*-band. Alternatively, the downlink frequencies can be derived from an onboard, radiation-hardened, temperature-controlled, ultrastable oscillator (USO) identical to the ones flown on Voyager (Eshleman *et al.*, 1977; Tyler, 1987). This latter

configuration is necessary for measurements of the atmosphere and ionosphere of Jupiter and for satellite occultations for two reasons. First, it is difficult to maintain a 2-way radio link with the spacecraft when signal strength and frequency exhibit dynamic variations as will occur in the Jupiter occultations. Second, the time delay in establishing a 2-way radio link after the downlink signal has been absent would result in a serious loss of data at emersion from the satellite occultations.

TABLE I  
Selected Galileo spacecraft radio system parameters (nominal)

	X-band	S-band
Transmitting parameters		
Frequency (MHz)	8415	2295
Wavelength (cm)	3.6	13.1
X/S coherency ratio	11/3	
Transmitting RF power (W)	12 or 21	9 or 27
4.8 m antenna gain (dBi)	50	38
Half-power beam width (deg)	0.6	1.5
Polarization	LCP or RCP	Linear
Axial ratio (dB)	2	32
Receiving parameters		
Frequency (MHz)	7167	2115
Wavelength (cm)	4.2	14.2
4.8 m antenna gain (dBi)	46	36
Polarization	LCP or RCP	Linear
Noise temperature (K)	270	1000
Ranging channel noise bandwidth (MHz)	1.5	

The Galileo radio system is enhanced relative to Voyager in three respects. First, the spacecraft can support ranging measurements not only in the conventional 2-way mode but also in a new differential downlink mode made possible by a tone generator on the spacecraft that can coherently modulate the *S*- and *X*-band downlink signals. Second, the spacecraft can receive uplink signals at both *S*- and *X*-band rather than *S*-band only. The ability to receive and coherently lock to an uplink signal at either frequency adds both redundancy and flexibility to the system and improves its scientific capabilities. As a result of a 20-year evolution in spacecraft radio equipment, Galileo is the first mission where the primary uplink and downlink communications will be conducted at *X*-band. This has made it possible to convert the *S*-band downlink from circular to linear polarization for scientific purposes (i.e., Faraday rotation measurements), the third enhancement relative to Voyager. With its strong magnetic field, Jupiter is a particularly good target for this type of measurement. Overall, these additions and modifications not only increase the speed and accuracy of command and data transmissions to and from the spacecraft but also advance the precision and scope of the science investigations.

The NASA Deep Space Network (DSN), operated by JPL, is responsible for tracking and commanding the spacecraft, receiving engineering and scientific telemetry, and for recording the basic measurements which become radio science data. It is a worldwide network of 70- and 34-m diameter antennas that are capable of simultaneously receiving and transmitting at *S*- and *X*-band in both left- and right-hand circular polarization (LCP and RCP, respectively). A hydrogen maser is used as a frequency reference for both the transmitted and received signals. Table II summarizes the expected performance of the DSN tracking stations. Figure 2 shows a partial block diagram of the relevant equipment. In addition, the 30-m antenna of the DLR located near Weilheim, Germany, has been subscribed for extensive tracking of Galileo during the interplanetary cruise phase.

TABLE II  
Selected DSN station parameters (nominal)

Antenna diameter (m)	70		34		34	
			Standard		High Efficiency	
Transmitting parameters	<i>S</i>		<i>S</i>		<i>X</i>	
Frequency (MHz)	2115		2115		7167	
Power (kW)	20/400		20		20	
Antenna gain (dBi)	63		55		67	
Polarization	LCP or RCP		LCP or RCP		LCP or RCP	
Receiving parameters	<i>X</i>	<i>S</i>	<i>X</i>	<i>S</i>	<i>X</i>	<i>S</i>
System noise temperature (K) (at zenith; typical)	21	17	25	21	20	38
Frequency (MHz)	8415	2295	8415	2295	8415	2295
Polarization	Simultaneous	Simultaneous			Simultaneous	
	LCP and RCP	LCP and RCP	LCP or RCP	LCP or RCP	LCP and RCP	LCP or RCP

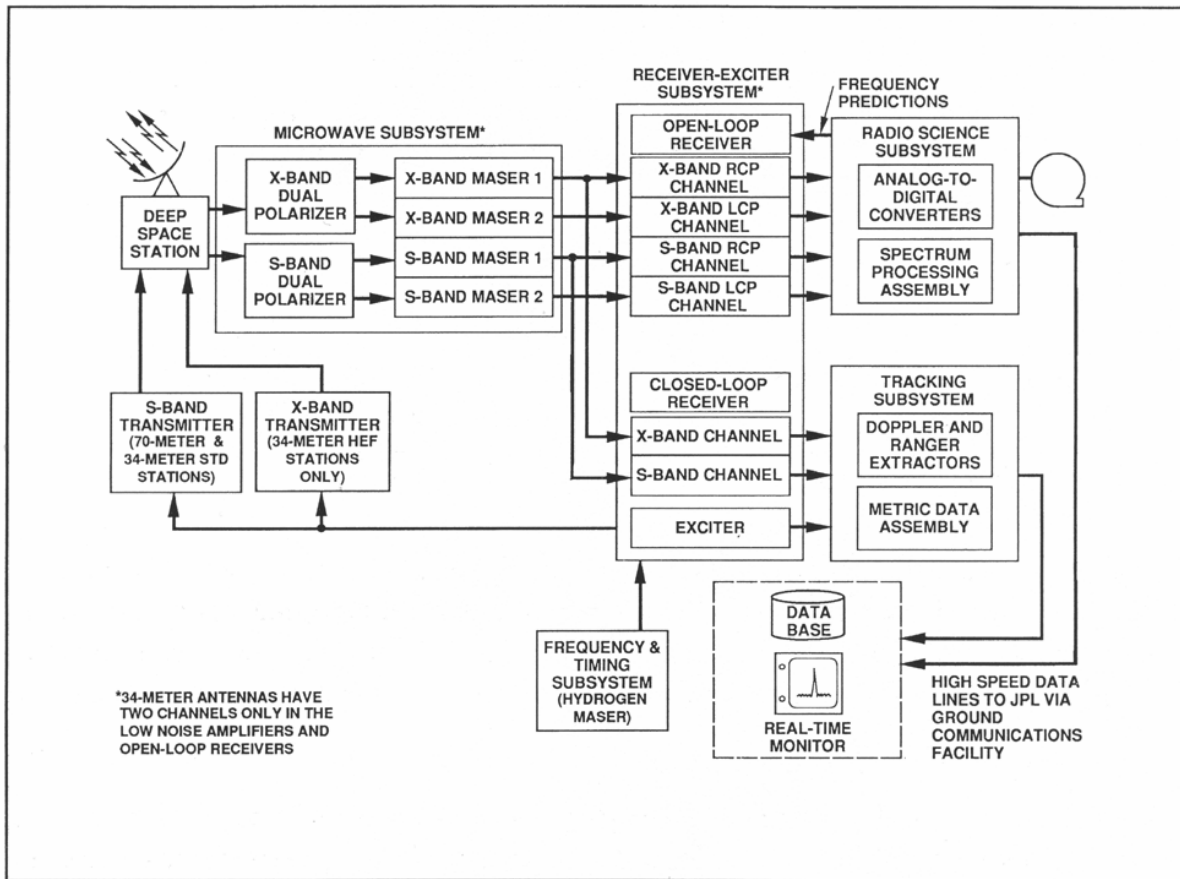


Fig. 2. DSN ground station functional block diagram for Galileo radio science.

The frequency stability of the radio link between spacecraft and Earth is a key parameter for many of the radio science experiments. The performance of the spacecraft USO and the hydrogen masers of the DSN can be characterized through use of the Allan variance (Barnes *et al.*, 1971); the square root of this quantity represents the size of a typical frequency fluctuation expressed as a fraction of the average frequency. Table III gives representative results on several time scales.

Procedures for recording radio science data at the DSN are mostly standard and will not be reviewed here. The reader should refer to the literature concerning radio science results from Voyager for further discussion.

## 2.2. MEASUREMENT TECHNIQUES

Neutral gases and magnetized plasmas distributed along the propagation path between the spacecraft and a ground antenna can distinctively influence some or all of the following properties of radio waves: phase velocity, group velocity, direction of travel, amplitude, and polarization. Variations in these propagation parameters lead in turn to changes in the characteristics of the signals received on Earth. The Galileo radio propagation experiments

involve measurements at a ground antenna of the frequencies of the two signals, differential phase, absolute and differential propagation time delay, signal strength, and polarization. The relationships between each parameter and the properties of the media provide the basis for remote sensing in these experiments.

TABLE III  
Performance characteristics of the USO and H<sub>2</sub> maser

	Integration time (s)	Frequency stability <sup>a</sup>
USO (spacecraft)	1	3 x 10 <sup>-11</sup>
	10	4 x 10 <sup>-12</sup>
	100	1 x 10 <sup>-12</sup>
	1000	1 x 10 <sup>-12</sup>
H <sub>2</sub> maser (ground stations)	1	2 x 10 <sup>-13</sup>
	10	3 x 10 <sup>-14</sup>
	100	4 x 10 <sup>-15</sup>
	1000	2 x 10 <sup>-15</sup>

<sup>a</sup> Square root of Allan variance (see text).

### 2.2.1. Frequency and Differential Phase

Any change in the number density of free electrons or of neutral gases along the propagation path between spacecraft and Earth will produce corresponding changes in the phase of a received signal. This effect produces an apparent Doppler shift in signal frequency. Moreover, the refractive index of a plasma depends strongly on frequency while that of a neutral gas generally does not for the frequencies considered here. By comparing phase measurements at two coherently-related frequencies, one can therefore distinguish between effects caused by neutral gases and those caused by plasmas. For example, the following phase difference is advantageous to studies of the solar corona as well as the ionospheres of Jupiter and its moons:

$$\delta\phi \equiv \Phi_S - \frac{3}{11} \phi_x \approx \frac{K_1}{f_s} \int_{\text{path}} N(S) ds$$

Where  $K_1 = 7.82 \times 10^{-7}$  (mks units).

Here,  $\varphi$  is phase,  $f$  is frequency, and the 's' and 'x' subscripts refer to the S- and X-band signals, respectively. To a good approximation, the combination  $\varphi_s - (3/11) \varphi_x$  removes from the data effects caused by neutral gases, relative motion of the spacecraft and ground antennas, and instability of the USO so that  $\delta\varphi$  is proportional to the number density of free electrons,  $N$ , integrated along the propagation path,  $s$ . We will refer to the path integral  $I = \int N(s) ds$  as the columnar electron content. While measurements of  $\delta\varphi$  can be used to monitor changes in  $I$ , an absolute measure of  $I$  cannot be obtained with this technique.

### 2.2.2. Absolute and Differential Propagation Time Delay

The time delay for signal propagation between spacecraft and Earth is obtained in the 2-way ranging mode by transmitting to the spacecraft a signal modulated by a ranging code. The coded signal received by the spacecraft is relayed back to Earth at the two downlink frequencies by the onboard transponders. The ground tracking station records the round trip propagation time as well as the difference between the arrival times of the range code at the two signal frequencies. Possible ambiguities in total range are resolved by transmitting the range code at several modulation frequencies. Alternatively, in the one-way ranging mode, ranging tones generated on the spacecraft are used to modulate the S- and X-band downlink signals. The tracking station records the difference in arrival times, yielding the differential but not the absolute range to the spacecraft.

Measurements of propagation time can be used for remote sensing because the propagation medium affects the group velocity of the radio signals. As with differential phase observations, the effect of a plasma on the group velocity is dispersive while the effect of a neutral gas is not. Consequently, the differential propagation time delay can be expressed as

$$\Delta\tau_{s/x} \equiv \tau_s - \tau_x \cong \frac{K_2}{f_s^2} I$$

Where  $K_2 = 1.25 \times 10^{-7}$  (mks units).

Here,  $\tau_s$  and  $\tau_x$  are the propagation time delays at S- and X-band, respectively.

Differential time delay data differ from differential phase data in that an absolute measure of  $I$  can be obtained from the former but not the latter. However, either can be used for observing changes in  $I$ . For propagation experiments with Galileo, the choice of techniques is dictated by the experiment geometry. Solar conjunctions last several weeks and involve the use of multiple ground tracking stations which rise and set sequentially as the experiment progresses. In this situation, differential range data are essential for minimizing problems arising from gaps in station coverage and for establishing boundary conditions for integrating differential phase data. On the other hand, occultations by planets and satellites involve characteristic changes in  $I$  over shorter time intervals, typically a few hours or less. As the repetition rate for range

measurements is constrained by practical considerations, observations of planetary or satellite occultations rely exclusively on measurements of differential phase.

### 2.2.3. Signal Strength

Variations in signal strength on both short and long time scales are important to several investigations. Radio-wave scattering in the solar corona as well as the atmosphere and ionosphere of Jupiter produces intensity fluctuations on short time scales, typically a few seconds or less. These observations are germane to studies of the small-scale structure and dynamics of these media. On somewhat longer time scales, ammonia - a trace constituent in the atmosphere of Jupiter - can cause a reduction in signal intensity through absorption. As this absorption is strongly dependent on frequency, the two-frequency capability is important for extending the dynamic range of the measurements.

### 2.2.4. Polarization

A linearly-polarized electromagnetic wave propagating through a magnetized plasma will experience a rotation in its angle of polarization (cf. Yeh and Liu, 1972). The equations governing this phenomena, which is known as Faraday rotation, depend on the frequency of the radio signal,  $f$ , relative to the characteristic frequencies of the plasma:

$$2\pi f_p = \left( \frac{Ne^2}{\epsilon_0 m} \right)^{1/2} \quad \text{and} \quad 2\pi f_B = \frac{eB}{m}$$

Here,  $e$  and  $m$  are the charge and mass of an electron, respectively,  $B$  is the magnitude of the magnetic field,  $\epsilon_0$  is the vacuum permittivity,  $N$  is the number density of free electrons,  $f_p$  is the plasma frequency, and  $f_B$  is the electron gyrofrequency. Under conditions where  $f \gg f_p$  and  $f_B$ , the angle of rotation of the polarization vector can be expressed as

$$\Omega \approx \frac{K_3}{f^2} \int_{\text{path}} N(s) \mathbf{B}(s) \cdot ds$$

Where  $K_3 = 2.36 \times 10^4$  (mks units).

The path of integration coincides with the path followed by the radio signal propagating from spacecraft to Earth,  $s$  is the distance measured along the path, and  $\mathbf{B}$  is the magnetic field vector. The Faraday data, when combined with the previously mentioned measurements of columnar electron content, can be used to infer a value for the magnetic field along the path through the plasma. Galileo is the first spacecraft to provide this capability.

The rotation of the Galileo spacecraft (and the high-gain antenna) at a rate of about 3 revolutions per minute causes an identical rotation with the appropriate time delay in the angle of polarization of the *S*-band signal received on Earth. Changes in  $\Omega$  arising from Faraday rotation appear superimposed on this rotating polarization vector. In practice, the DSN does not directly measure the angle of polarization; instead, the *S*-band signal is received and recorded simultaneously in coherent RCP and LCP channels so that polarization information can be extracted. The data are then calibrated to remove the effect of spacecraft rotation through use of engineering telemetry received from the spacecraft.

### 3. Solar Corona

The solar corona experiments are performed for several weeks around Galileo's superior conjunctions, i.e., when the spacecraft is on the opposite side of the Sun from the Earth. In this configuration the radio signals propagating between Earth and spacecraft traverse the solar atmosphere. The radio signals are scattered and refracted as they propagate through the hot, tenuous, turbulent plasma of the solar corona. These effects are responsible for degradation of command transmission on the uplink and high bit error rates in the data reception on the downlink. On the other hand, they intrinsically yield valuable information about the structure and dynamics of the solar corona. Coronal sounding investigations using the polarization and group delay characteristics of radio signals from spacecraft in solar occultation have been performed for many years (Bird, 1982; Bird and Edenhofer, 1990) and such an experiment will be carried out during the cruise phase of the Ulysses mission (Volland *et al.*, 1983). Similarly, scintillation and scattering techniques for observing the corona and interplanetary medium have become well developed and have produced results on bulk motion and accretion in the corona, the variation of electron density irregularities with solar cycle and distance from the Sun (Tyler *et al.*, 1981; Woo and Armstrong, 1979, 1981; Woo, 1988), the evolution of interplanetary disturbances, and coronal mass ejections (Woo *et al.*, 1982, 1985).

Although the Galileo mission is not primarily concerned with solar research, its interplanetary trajectory and radio system capabilities are well suited for coronal radio sounding investigations. Table IV gives the timing and geometrical parameters of the four Galileo superior conjunctions en route to Jupiter. The Galileo orbital geometry at each of the conjunctions is shown in Figure 3.

#### 3.1. SCIENTIFIC OBJECTIVES

The Galileo Solar Corona Experiment (SCE) will use a variety of radio sounding techniques for investigations of the otherwise practically inaccessible regions of the outer solar atmosphere. Whereas observations of the solar corona at optical wavelengths (e.g., with coronagraphs) are generally possible only out to a few  $R_o$  ( $R_o$  = solar radius), radio sounding experiments can be employed with good results out to 40  $R_o$  and beyond. In this way such methods can at least partially bridge the gap between the in-situ measurements of previous spacecraft in to about 60  $R_o$  and the optical observations in the immediate neighborhood of the Sun.

Specific scientific objectives of SCE include investigations of the following:

- The 3D-electron density distribution of the coronal plasma, and its relation to the photospheric magnetic field configuration as obtained from solar magnetograms.
- The structural differences between coronal holes ('open' magnetic configurations), active regions (presumably 'closed' magnetic field lines), and the 'quiet' Sun (open or closed ?)
- Characteristics of the acceleration regions of the solar wind in coronal holes, streamers, and other parts of the corona.
- Coronal characteristics possibly related to the heating agent responsible for driving the temperature of the solar material from some  $10^4$  K in the chromosphere to over  $10^6$  K in the corona.
- The effects of resonant solar oscillations on the dynamical characteristics of the , relatively tenuous solar atmosphere.
- The excitation and propagation conditions for various types of plasma waves, e.g., Alfvén waves, magnetoacoustic waves, etc.
- The distribution of electron density irregularities over a wide range of spatial scale sizes and their variation with solar cycle, solar distance, and latitude.
- The topology and evolution of interplanetary disturbances near the Sun and their relationship to white-light coronal mass ejections.

TABLE IV  
Galileo solar conjunctions based on actual VEEGA orbit

Sup. conj. No.	Solar proximate date	Proximate <sup>b</sup> solar offset ( $R_0$ )	Mean daily motion ( $R_0$ day <sup>-1</sup> )	East limb ingress <sup>c</sup> $2^\circ < R < 8^\circ$ One 70-m day <sup>-1</sup>	Center occultation $R < 2^\circ$ 70-m continuous	West limb egress $2^\circ < R < 8^\circ$ One 70-m pass day <sup>-1</sup>	S/C range (AU)
$C_1$	22 Jan., 1992	8.4 N	2.05	9-22 Jan. (14) days	None	23 Jan.-6 Feb. (15 days)	3.25
$C_2$	3 Nov., 1993	2.5 S	2.57	22-30 Oct. (9 days)	31 Oct.-6 Nov. (7 days)	7 Nov.-14 Nov (8 days)	4.38
$C_3$	1 Dec., 1994	0.5 S	2.97	21-27 Nov. (7 days)	28 Nov.-3 Dec. (6 days)	4 Dec.-11 Dec. (8 days)	5.96
$C_4$	19 Dec., 1995	0.9 N	3.03	9-15 Dec. (7 days)	16-21 Dec. (6 days)	22-28 Dec. (7 days)	6.26

<sup>a</sup> Values for  $C_4$  are only approximate - Jupiter arrival data is 7 December, 1995.

<sup>b</sup> (N/S) = north/south pole crossing.

<sup>c</sup> Solar offset  $R$ :  $2^\circ \cong 7.5 R_0$ ;  $8^\circ \cong 30 R_0$ .

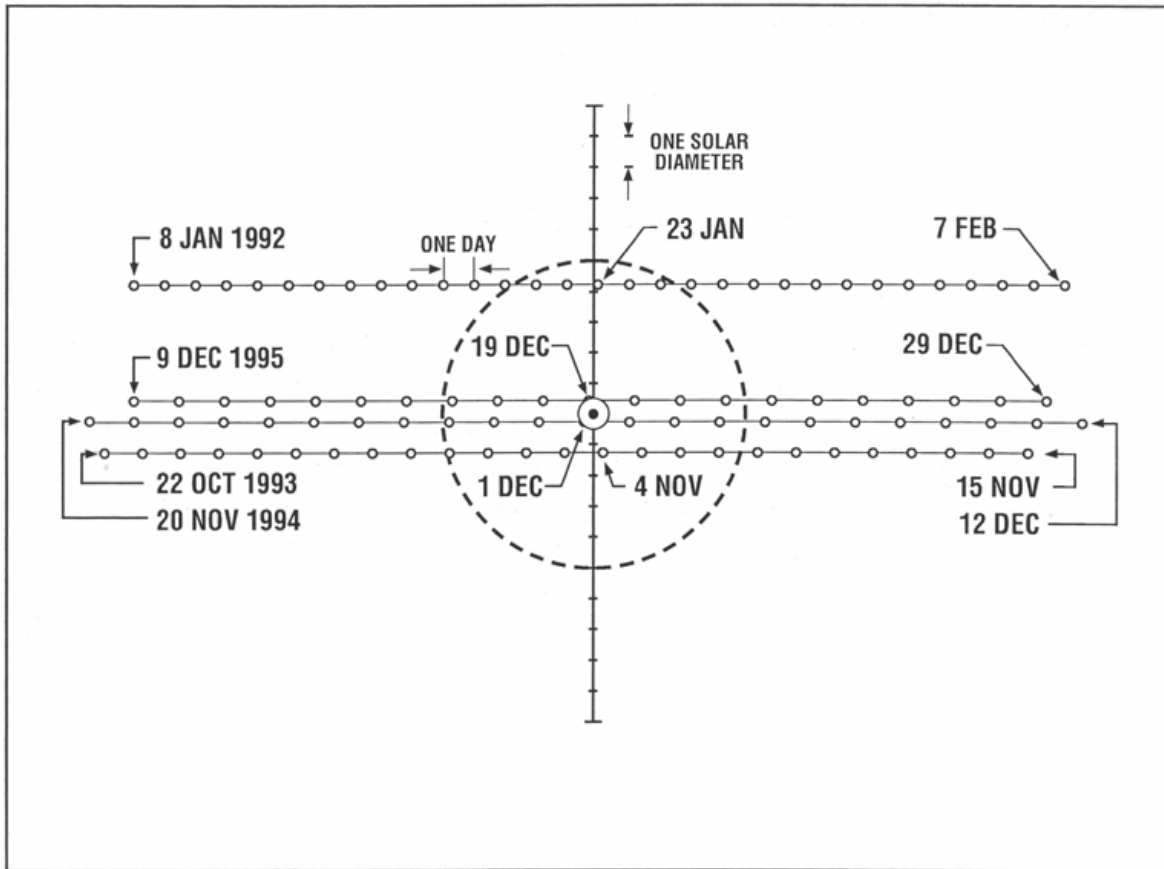


Fig.3. View from Earth of the four solar conjunctions of the Galileo spacecraft (cf. Figure I). The circle in the center is the solar disk; the dashed circle has a radius of  $10 R_{\odot}$ . Spacecraft position at 00:00 UT each day is shown by small circles. Axis ticks are separated by  $2 R_{\odot}$ .

The Galileo SCE, exploiting the Faraday capability as one specific example of meeting the above objectives, will place particular emphasis on achieving a better understanding of magnetic fields in the solar corona. It is anticipated that the magnetic field measurements obtained with Galileo will verify previous results for the background coronal field (Pätzold *et al.*, 1987) without recourse to independently derived coronal density models. An equally important aspect of these observations would be the unprecedented advantage of separating magnetic from electron density fluctuations in order to assess the spatial/spectral distribution of coronal MHD-wave activity. There exists strong evidence, based on previous Faraday/electron content data, that the magnetic fluctuations are dominant (Hollweg *et al.*, 1982). Finally, should we be fortunate enough to witness the transit of a coronal mass ejection through the spacecraft's signal ray path, the Galileo SCE measurements would be ideal for testing the alleged role of the magnetic field as a driving force for these poorly understood solar phenomena. An earlier analysis of the few rare and only partially observed examples was inconclusive (Bird *et al.*, 1985).

### 3.2. EXPERIMENTAL OBSERVATIONS

The three main experiments to be conducted during solar superior conjunctions are:

#### *Faraday, Doppler, and Range*

The Galileo radio propagation experiment will be the first to utilize Faraday rotation plus dual-frequency range and range-rate measurements, thereby enabling a direct estimate of the coronal magnetic field. Faraday rotation is sensitive only to the mean line-of-sight component of the magnetic field  $\langle B_L \rangle$ , as weighted by the plasma density. The complex solar field can result in cancellation effects along the signal ray path so that very little rotation is sometimes observed even at small solar elongations. Nevertheless, the strength and orientation of the coronal magnetic field can often be approximated under appropriate and reasonable assumptions (Volland *et al.*, 1977; Pätzold *et al.*, 1987). A simple 'rule of thumb' formula for the mean longitudinal magnetic field in the corona (in gauss) can be written as

$$\langle B_L \rangle \cong \frac{\Omega}{\Delta\tau_{s/x}}$$

where  $\Omega$  is given in degrees at S-band, and  $\Delta\tau_{s/x}$  is given in ns. Plasma differential delay times of up to a few tens of thousands of nanoseconds have been measured in previous solar conjunctions (1 ns  $\cong 4 \times 10^{16}$  el m<sup>2</sup> for the S/X-band system).

#### *Multiple Ground Station Observations*

Whenever two or more ground stations are tracking simultaneously, a cross correlation of the signal fluctuations observed at the different ground stations can be used to compute a pattern velocity, which then can be related to the bulk velocity of coronal plasma or the phase velocity of a plasma wave. Any signal parameter can be used for this purpose. An example of the Faraday rotation fluctuations observed at two widely separated DSN ground stations during a solar occultation of Helios in 1983 (Bird *et al.*, 1985) is shown in Figure 4. Very large pattern velocities both away from and toward the Sun are often derived from these correlations, suggesting the presence of inward and outward propagating coronal Alfvén waves.

#### *Scintillation at S- and X-Band*

These investigations are based on radio scintillation and scattering techniques, with the observed scattering phenomena including amplitude scintillations, phase scintillations, and spectral broadening. Near-Sun observations will contribute to our understanding of electron density irregularities over 5 decades of spatial size scales (Woo and Armstrong, 1919).

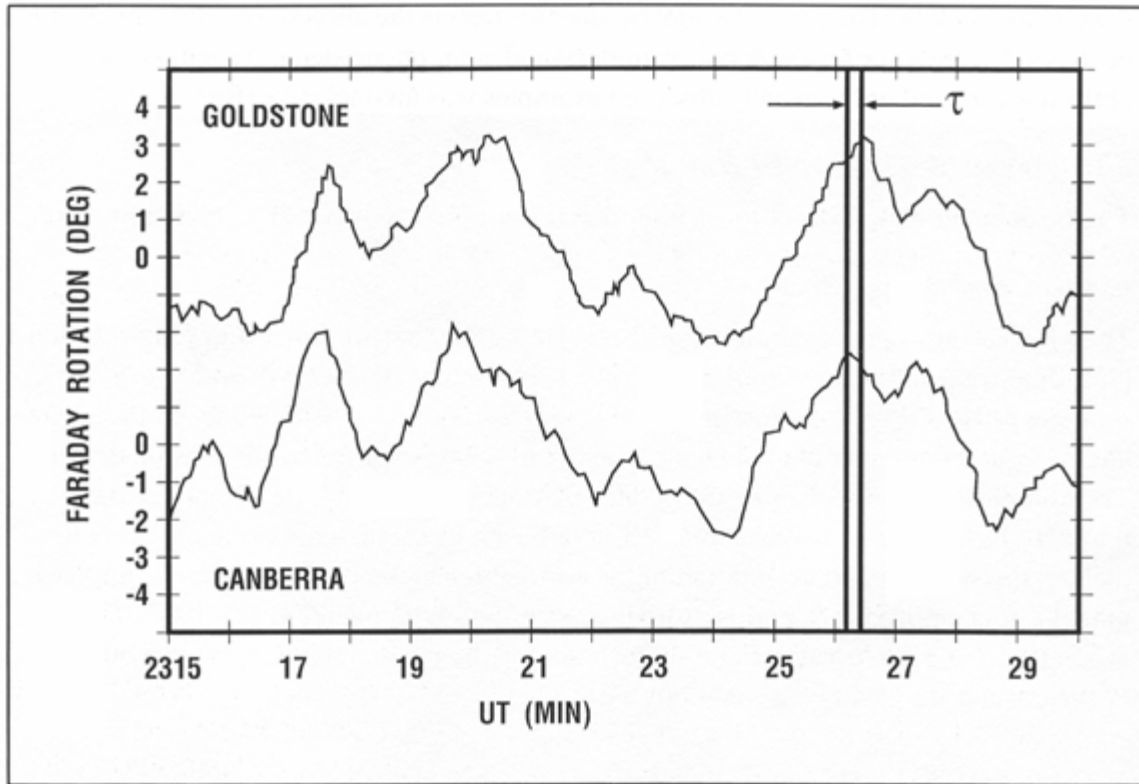


Fig.4. Helios Faraday rotation measurements recorded at the widely separated Goldstone (California) and Canberra (Australia) ground stations on 9 January, 1983. The radial separation of the ray paths from Helios to the two ground stations in the corona was  $\approx 2000$  km. In this case the time lag  $\tau = 10.6$  s (correlation coefficient = 0.93) yielded a radially outward pattern velocity of ca.  $200 \text{ km s}^{-1}$ . Other examples could only be explained by pattern velocities moving toward the Sun - a possible indicator of MHD waves.

#### 4. Jupiter and Satellite Occultations

Upon arrival at Jupiter in December of 1995, Galileo first has a close flyby of Io with no occultation and then spends about an hour collecting telemetry from the Probe as it enters the Jovian atmosphere. The Probe has an ultrastable oscillator which makes it possible to use the Doppler data from the Probe-to-Orbiter  $L$ -band link to characterize the entry path winds. A companion paper describes this experiment (Pollack *et al.*, 1992). Scintillations in the amplitude of the Probe-to-Orbiter radio signal will also be used to study small-scale irregularities and dynamics of Jupiter's atmosphere (Woo *et al.*, 1980).

The next event is a retropropulsion motor burn which injects Galileo into a 230-day orbit. The 1989 launch opportunity provided a particularly favorable geometry for obtaining Jupiter occultations which will occur on more than half of the planned orbits. At the time of writing this paper (1991) the tour selection process had not been started. Tour design begins in 1992, involves a number of operational and scientific trade offs and has the goal, from the radio

science perspective, of producing multiple occultations of the spacecraft by Jupiter and Io along with close flybys of and occultations by Europa, Ganymede, and Callisto. The orbit of the Galileo spacecraft is also expected to provide numerous opportunities for differential Doppler measurements concerning the spatial structure and temporal variations of the Io plasma torus.

#### 4.1. ATMOSPHERE AND IONOSPHERE OF JUPITER

The Galileo radio occultation experiments can provide the data needed to derive vertical profiles of refractivity and absorptivity in the neutral atmosphere at a quality comparable to that obtained from the corresponding experiments with Voyager (Eshleman et al., 1977; Lindal *et al.*, 1981, 1985, 1987; Tyler, 1987). However, Galileo's multiple occultations will be at various latitudes and will occur over an extended period of time. This makes it possible to study atmospheric properties in a more comprehensive manner and over a wider range of conditions than could be accomplished with Voyager. In this way the Galileo radio occultations can extend the Voyager results and contribute to a better understanding of Jupiter in several key areas.

To be successful, the radio occultation experiments with Galileo will require precise control of the orientation of the spacecraft antenna. Each experiment must include a spacecraft maneuver designed so that the antenna beam tracks the virtual radio image of Earth as it moves along the limb of Jupiter (as seen from the spacecraft). More specifically, the pointing direction of the antenna will be carefully controlled so as to yield the strongest possible signal at the tracking antennas of the DSN after refraction in the atmosphere of Jupiter.

Multiple occultations and global coverage could be of particular importance for providing measures of atmospheric ammonia, as derived from absorptivity profiles. One of the four Voyager occultations produced a profile of ammonia vapor abundance with very good height resolution, from about the 400 mb level where the concentration is limited by saturation to a few parts per million, to the condensation level which occurred near 900 mb, and on downward to the one bar pressure level where the mixing ratio was  $220 \pm 80$  ppm (Lindal *et al.*, 1981). That is, the measurement extended below the ammonia cloud base and thus reflects the composition of the lower well-mixed regions of the atmosphere. With Galileo it may be possible to extend such vertical profiles of the ammonia mixing ratio to global coverage. Other remote-sensing measures of the global distribution of ammonia, based on observations of thermal emission, do not provide fine height resolution and suffer from some ambiguity due to possible horizontal variations in temperature. Thus the radio occultation profiles and the global thermal emission measures are complementary in terms of coverage, resolution, and accuracy.

The scientific significance of these measures of ammonia can be summarized as follows. The abundance of ammonia on Jupiter is a consequence of the conditions in the primitive solar nebula, the process of planet formation, and the subsequent evolution of Jupiter over its lifetime. Several phenomena, acting at a variety of atmospheric pressures, determine the present spatial distribution of ammonia within the planet. These include photochemistry in the stratosphere, condensation in the upper troposphere, and at progressively deeper levels of the troposphere, chemical reactions with hydrogen sulfide and dissolution in water clouds. Vertical transport through convection and eddy mixing as well as large-scale atmospheric motions act to couple the effects of these various processes. Hence, global measurements of the abundance of ammonia

and its horizontal and vertical variations are key to understanding not only a variety of atmospheric phenomena but also the origin and evolution of the planet.

Favorable occultation geometries will be required for Galileo to accomplish the desired ammonia measures. The single profile of ammonia abundance described above was obtained during egress of Voyager 1 and applies to the equatorial atmosphere. Absorptivity profiles could not be derived from the other three Voyager occultations due either to the geometrical conditions (grazing occultation and large limb-spacecraft distances) or to very weak and Doppler-spread signals (Lindal *et al.*, 1981). It is not clear what fraction of the Galileo occultations will allow determination of accurate absorptivity profiles, but careful attention to experiment design, orbital trajectories, spacecraft antenna orientation, and signal measuring and processing techniques will be required to optimize results. In this regard, it is inherent that the region we wish to measure, extending in particular to below the cloud base, is of course the same region where the signal is being strongly absorbed to the point of extinction. The margin between the pressure levels at the cloud base and at signal loss was very small for the successful Voyager example, and can never be large for Galileo. Nevertheless, the potential importance of the ammonia measurements merits special attention to ameliorate the difficulties.

Another area where a multiplicity of atmospheric profiles is needed is for the study and characterization of the spatial and/or temporal variability of the stratosphere. For example, the near-equatorial profiles of the stratosphere from Voyager 1 exhibit temperature oscillations with an amplitude of about 10 K and a vertical scale of about 3 pressure scale heights. The vertical variations in temperature are similar in appearance at ingress and egress but about 180° out of phase at the two locations. Such effects are absent from the mid-latitude profile of the stratosphere obtained with Voyager 2. Moreover, Voyager images of the equatorial atmosphere show a periodic pattern of cloud plumes encircling the planet at 8° N latitude with a zonal wave number of about 12. Allison (1990) showed that both sets of observations could be interpreted consistently as manifestations of a Rossby wave that propagates in the vertical and zonal directions but remains confined in latitude near the equator. His results have wide implications for atmospheric phenomena ranging from the eddy mixing of the middle atmosphere to the structure of the water cloud (and the abundance of water vapor) in the deep troposphere, as well as the dynamical coupling between the troposphere and stratosphere.

Against this background, the Galileo radio occultations can contribute to a more comprehensive investigation of planetary-scale equatorial waves on Jupiter. In distinction to the ammonia measurement, accurate stratospheric profiles between about 1 and 100 mb are expected to be obtained from every occultation of Galileo. Each occultation measurement at latitudes between about 15° N and 15° S, where wave amplitudes are expected to be appreciable, will yield a snapshot of the vertical structure of the wave, allowing measurements of amplitude and vertical wavelength. Intercomparison of measurements at different locations, especially ingress and egress of the same occultation, will provide strong constraints on zonal wave number and meridional structure ( cf. Hinson and Magalhães, 1991 ). Coordinated observations of zonally periodic cloud structure with the imaging instrument on Galileo will complement this aspect of the radio science investigation, providing independent estimates of zonal wave number and, possibly, zonal phase speed. These coordinated observations, when combined with *in-situ* measurements by the Galileo Probe of the vertical structure and composition of the equatorial

atmosphere, can provide a far more complete picture of the behavior of equatorial waves on Jupiter, possibly allowing identification of the mechanism by which they are generated as well as assessment of their contribution to the energy and momentum budgets and eddy mixing of the middle atmosphere.

More generally, the Galileo refractivity profiles (extending from about 1 mb to 1 bar) will be used to search for latitudinal variations at all locations accessible to occultation measurements, and to refine the precision to which lapse rates can be determined. Accurate lapse rates in the troposphere could be used, for example, to help guide studies of the role of ortho-para conversion of molecular hydrogen in affecting atmospheric dynamics and stability (Gierasch and Conrath, 1985). Both tropospheric and stratospheric profiles as measured by radio occultation will also be used in conjunction with infra-red temperature sounding to refine the precision to which the atmospheric helium abundance can be deduced through intercomparisons (cf. Conrath *et al.*, 1984, 1987).

In all of the atmospheric studies described above, particular emphasis will be placed on comparison with results from the Galileo Probe experiments. The *in-situ* measurements will be used to calibrate and anchor the radio experiments for application to other regions of Jupiter, and in addition, to the other major planets where radio but no probe measurements have previously been made.

For the ionosphere of Jupiter, it is again the multiplicity and global coverage provided by the Galileo radio occultations that are of special significance. Profiles in height of the electron number density of the ionospheric topside have been obtained from both the Voyager and Pioneer encounters with Jupiter, but even though the Voyager radio instrumentation is generally more capable, the shorter limb-spacecraft distance in the Pioneer 10 and 11 encounters was fundamental in making possible a characterization of the very sharp, multiple, dense, low-lying (below 1000 km altitude as measured from the 1 bar pressure level) layers of the ionosphere at the occultation locations (Fjeldbo *et al.*, 1975, 1976a, b). This experience emphasizes the importance of designing the Galileo orbital tour so that at least some of the Jupiter radio occultations involve relatively short planet-spacecraft distances. The sharp low-lying layers of ionization are poorly understood and yet appear to be a general property of giant planet ionospheres, since they are also observed at Saturn, Uranus, and Neptune (Lindal *et al.*, 1985; 1987; Tyler *et al.*, 1989). From the greater areal and temporal coverage on Jupiter provided by Galileo, it may be possible to characterize the horizontal extent and temporal variations of the layers as clues to divining their source and other characteristics. The topside of the main ionization layer on Jupiter (which extends to at least 4000 km above the 1-bar pressure level) apparently consists of atomic hydrogen as the principal ion. The plasma temperature of more than 1000 K may exceed the local temperature of the neutral species by about a factor of two. Lower down in the main layer, other ions and chemistry must play a role in determining the plasma density (e.g., see Horanyi *et al.*, 1988). The experimental results concerning the topside are now too sparse to investigate effects on the ionosphere of variations in solar activity, solar zenith angle, magnetospheric characteristics such as the Io torus, and position on Jupiter. Galileo radio occultations could fill at least some of the gaps in our knowledge.

For both the ionosphere and neutral atmosphere, the Galileo radio measurements will provide information not only about the profiles discussed above, but also about small-scale structures embedded within these regions. They manifest themselves in the form of scintillations of both the signal amplitudes and phases. The purpose of this investigation of the neutral atmosphere of Jupiter is to characterize the scintillations and deduce information on the global and spatial wave number distribution of temperature irregularities of scale sizes smaller than several kilometers. The goal is to interpret the results in terms of small-scale atmospheric dynamical processes, including but not restricted to turbulence and gravity waves (Woo *et al.*, 1980; Hinson and Tyler, 1983), and to infer estimates of vertical transport (Woo and Ishimaru, 1980; Hinson and Magalhães, 1991). For the ionosphere of Jupiter (and of satellites for which an ionosphere is detected), the investigation will be of the global morphology of scintillations and magnetic field orientation in the ionosphere, and the variation with altitude and latitude of the magnitude and spatial wave number spectrum of the electron density irregularities for scale sizes smaller than several kilometers (Woo and Yang, 1978; Woo and Armstrong, 1979; Hinson and Tyler, 1982; Hinson, 1984). These ionospheric measurements will lead to a better understanding of the nature and production mechanisms of the electron density irregularities, the interaction of the solar wind and magnetosphere with the ionosphere, and the configuration of the magnetic field near the planet.

#### 4.2. SATELLITE OCCULTATIONS

Another aspect of the Galileo radio propagation experiments concerns the study of Jupiter's satellites. As in the case of previous missions to the outer planets, radio tracking data acquired during the spacecraft's occultation by a satellite will be used to determine the satellite's diameter and, possibly, the properties of its atmosphere and ionosphere.

Measurements of satellite diameters involve the use of spacecraft and satellite ephemerides and the limb diffraction effects observed during ingress and egress. The accuracy of the measurements, which depends on the occultation geometry and the accuracy of orbit determination, should be about 1 km if the results from earlier missions can be used as a guide.

Integral inversion of the differential Doppler data acquired during ingress and egress, may provide information on the vertical distribution of free electrons. The detection limit for plasma in a satellite ionosphere ranges from  $10^8$  to  $10^{10}$  electrons per cubic meter depending on the extent to which the radio link is also affected by phase variations produced by plasma in the interplanetary medium and the terrestrial ionosphere. The neutral gas number density may in turn be inferred from the data on the vertical electron distribution - or, if the gas density is of the order of  $10^{10}$  molecules per cubic meter or greater, directly from phase perturbations observed during ingress and egress.

The neutral gas detection limit for the phase data to be acquired with the Galileo radio system is comparable to that of Voyager 2, which was used to characterize the atmosphere of Triton whose surface gas density was determined to be  $2.2$  to  $2.6 \times 10^{21}$  molecules per cubic meter (Tyler *et al.*, 1989). The gases near the surfaces of the Jovian satellites may be too tenuous for direct measurements by radio occultation. However, a substantial ionosphere has been observed on Io by Pioneer 10 (Kliore *et al.*, 1975), and differential phase data permit inferences to be made

about atmospheric regions where the gas density is much lower than  $10^{20}$  molecules per cubic meter. For example, the peak electron concentration in Triton's ionosphere was detected with the Voyager radio link at an altitude where the gas density is only about  $10^{16} \text{ m}^{-3}$ , and dispersive phase measurements conducted during Mariner 10's occultation by Mercury (Howard *et al.*, 1974) have yielded an upper limit for the gas density near Mercury's surface of  $10^{12} \text{ m}^{-3}$  (Fjeldbo *et al.*, 1976b).

The vertical profiles of electron number density obtained with Pioneer 10 have helped to anchor theoretical models of the atmosphere of Io (e.g., Kumar, 1985; Ingersoll, 1989). Nevertheless, we assign a high priority to obtaining new radio occultation measurements of the ionosphere of Io for the following reasons. Given the substantial improvements in the instrumentation of Galileo relative to Pioneer 10, occultation experiments with Galileo can yield more accurate ionospheric profiles leading to improved constraints for the theoretical models. Moreover, repeated occultations at a variety of phases in the orbit of Io would provide valuable results concerning the spatial and temporal variability of Io's atmosphere and its interaction with the magnetosphere. These results would contribute to an improved understanding of the meteorology and aeronomy of this unique solar system satellite.

#### 4.3. THE IO PLASMA TORUS

Radio science experiments with Galileo can contribute to a better understanding of the Io plasma torus, a structure of considerable significance to the behavior of the Jovian magnetosphere (e.g., Connerney, 1987). When the radio link between spacecraft and Earth traverses the torus, free electrons will induce dispersive Doppler shifts on the dual-frequency radio signals. These data will provide a measure of the total number of free electrons integrated along the path of propagation with an accuracy comparable to previous results obtained with Voyager (Levy *et al.*, 1981). The integrated electron content in turn provides useful constraints on the spatial structure of the torus. With the frequent opportunities for such measurements afforded by an orbiting spacecraft, these radio science results will complement the *in-situ* measurements obtained during the flight of Galileo through the torus immediately prior to orbit insertion as well as remote observations of the torus with other instruments on Galileo.

#### 4.4. JUPITER'S MAGNETIC FIELD

The unique combination of radio equipment on the Galileo spacecraft makes possible for the first time Faraday rotation measurements concerning the strength and configuration of the internal magnetic field of Jupiter. We plan to exploit this capability to investigate the characteristics of the magnetic field in the ionosphere of Jupiter - a region that remains inaccessible to *in-situ* measurements.

The Faraday rotation experiment will be conducted during all occultations of the spacecraft by Jupiter that occur during the orbital tour. Each occultation presents two good opportunities for Faraday rotation measurements, one near immersion and the other near emersion. During these time intervals, the path followed by the radio signals propagating from spacecraft to Earth passes through the topside ionosphere of Jupiter but remains above the neutral atmosphere. For example, Figure 5 shows the view from Earth of the initial occultation by Jupiter that

immediately follows orbit insertion. Faraday rotation measurements during this event will allow remote sensing of the ionosphere and magnetic field at two locations, both at mid-latitudes in the southern hemisphere. Thus the scope of this investigation of the magnetic field will be determined by the total number and the locations of the occultations by Jupiter, which are a direct consequence of the geometry of the orbital tour.

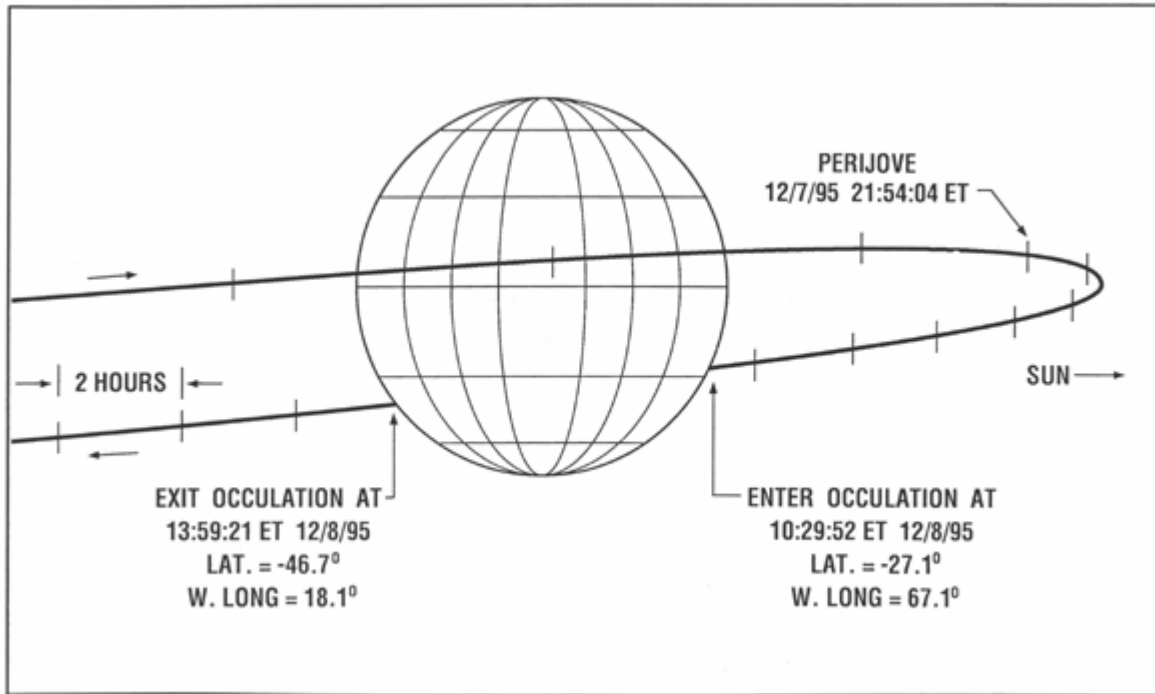


Fig.5. View from Earth of the initial occultation of the Galileo spacecraft by Jupiter (provided by J. R. Johannesen of the Galileo Navigation Team). Distance from spacecraft to Jupiter is about  $12 R_J$  at immersion and  $14 R_J$  at emersion, where  $R_J$  is the radius of Jupiter.

In an earlier section we gave a formula for the angle of rotation of the polarization vector,  $\Omega$ , that results from Faraday rotation. (This approximate formula is valid in the ionosphere of Jupiter where  $f_p \leq 4$  MHz and  $f_B \leq 40$  MHz, so that  $f_s \gg f_p$  and  $f_B$ .) Several conclusions follow from this expression for  $\Omega$ . First,  $\Omega$  depends only on the component of  $\mathbf{B}$  that is parallel to the direction of propagation. For the geometry of the Galileo orbit and the inclination of the spin axis of Jupiter (cf. Figure 5)  $\Omega$  thus responds most directly to  $B_\phi$ , the longitudinal component of Jupiter's magnetic field. Second,  $B_\phi$  cannot be inferred from  $\Omega$  without independent measurements of  $N$ , the number density of the free electrons. We will obtain these through measurements of differential phase,  $\delta\phi$ , as described previously. The combined measurements of  $\Omega$  and  $\delta\phi$  will allow inferences of  $B_\phi$ .

When properly normalized, the ratio  $\Omega/\delta\phi$  gives the value of  $B_\phi$  averaged along the path of integration with  $N$  acting as a weighting function. This is the basic result of the Faraday rotation measurements. The effective length of the path of integration is approximately the geometrical mean of the circumference of the planet and the scale height of the topside ionosphere:

$$L_{\text{eff}} = \sqrt{2\pi RH}$$

For the ionosphere of Jupiter,  $R \cong 74,000$  km at the equator (Lindal *et al.*, 1981) and  $H \cong 900$  km (Eshleman *et al.*, 1979a, b) so that  $L_{\text{eff}} \cong 2 \times 10^4$  km, equivalent to about  $16^\circ$  in latitude at the equator. This represents the effective spatial resolution of the experiment.

We conducted numerical simulations to evaluate the potential of the Faraday rotation measurements. These involved a model for the ionosphere based on Voyager radio occultation measurements (Eshleman *et al.*, 1979a, b) along with a variety of models for the internal magnetic field which have been derived from Pioneer and Voyager magnetometer data (e.g., Acuna and Ness, 1976; Connerney *et al.*, 1982; Connerney, 1987). From these calculations we anticipate that Faraday rotation measurements with Galileo will yield results in the range  $-\pi < \Omega < \pi$  (radians). The value of  $\Omega$  depends strongly on the location of the measurements as a result of the complex structure of the magnetic field near the planet. Of greater significance, the differences among competing models of Jupiter's magnetic field result in variations in  $\Omega$  of order  $\pi/10$ , which represents the accuracy in measurements of  $\Omega$  required to obtain essentially new information about the magnetic field configuration. We have designed the experiment with the goal of exceeding this threshold of sensitivity by a factor of at least ten. At this level of performance, Faraday rotation measurements are highly complementary to magnetometer measurements for investigating the internal magnetic field of Jupiter.

## 5. Bi-Static Radar Studies of the Icy Galilean Moons

The Galileo mission provides the first opportunity to obtain critical angular data on the electromagnetic scattering properties of the surfaces of the icy Galilean moons of Jupiter. Ground-based radar measurements of Europa, Ganymede, and Callisto indicate that they may share surface and subsurface properties that are currently not understood, but which produce back scatter echoes that differ profoundly from those obtained from rocky planets and moons. Preliminary radar studies of Titan and the south polar cap of Mars suggest that these surfaces may be similar to the icy moons in this regard. More complete understanding in this area is important and possibly vital for the design and interpretation of radar mapping missions to icy planets and moons (particularly Titan), and for improved understanding regarding the formation, evolution, and current state of outer-solar-system surfaces. In a possibly related development, new insight on this subject could follow from recent experimental and theoretical studies of the three bodies of our solar system (Mars, Triton, and Pluto) that appear to have sensible atmospheres whose main gaseous constituent is also present on the surface as ice.

Monostatic radar echoes from the icy Galilean moons are unusually strong with anomalous polarizations and Doppler spreads, as compared with echoes from the terrestrial planets and Earth's moon (Goldstein and Morris, 1975; Campbell *et al.*, 1978; Ostro *et al.*, 1980; Ostro, 1982). For example, the normalized backscatter radar cross section of our rocky moon is about 0.1, while, for icy Europa, it is 2.6 for echoes of all polarizations. For reference, the corresponding number for a perfectly reflecting sphere is 1.0.

For a circularly polarized incident wave, about 90% of the echo energy is in the expected circularly polarized sense for our moon, and the order of 10% is in the opposite or unexpected sense. For a perfectly reflecting sphere, the corresponding numbers are 100% and zero. For Europa, they are about 40% and 60%, respectively, so that most of the energy has the unexpected Polarization. Linearly polarized incident waves are also anomalously depolarized by the Icy Galilean moons.

For a homogeneous sphere, backscattered surface reflections come only from the center of the disk, since off-normal incident rays are scattered in other directions. Although rocky-planet echoes are mainly from this central zone, the icy-moon echoes are strong from nearly all areas of the disk. Thus, by comparison, the limbs appear to be remarkably bright when observed by radar so that the Doppler spreads of the echoes are unusually large.

The recent reports of the detection by Earth-based radar of echoes from the south polar cap of Mars (Muhleman *et al.*, 1989) and from Titan (Muhleman *et al.*, 1990) describe the echoes as being unusually strong with the suggestion that they may have characteristics similar to the returns from the icy Galilean moons of Jupiter. Thus the evidence is strong and growing that the icy surfaces that occur in the outer solar system may share common attributes that are not now understood, but which are fundamental to the way in which these surfaces interact with electromagnetic waves.

A number of theories have been proposed to account for these observations (Ostro and Pettingill, 1978; Goldstein and Green, 1980; Hagfors *et al.*, 1985; Eshleman, 1986a, b, 1987; Gurrola and Eshleman, 1990; Ostro and Shoemaker, 1990; Hapke, 1990). It is generally agreed that the scattering is not just from surface structures but must involve significant penetration of the radio photons to at least meters below the surface, and possibly to a few tens of meters. Cold ice has a low electromagnetic loss tangent so that if the near-surface regions are relatively pure ice, such penetration need not involve significant absorption. The strong backscatter echoes argue for a mechanism that can change photon directions over large angles with efficiency and with significant areas of coherence. Although not common to all theories, several invoke the phenomenon of total internal reflection at dielectric interfaces for such efficiency and coherence. Furthermore, even if every incident photon were returned to space, the observed globally-integrated echo strengths (at least for Europa and Ganymede) require that they display some preference for returning along the direction from which they arrived. They might simultaneously favor another direction, such as the specular one relative to the surface, but from conservation of energy it follows that the backscatter direction must involve stronger scattering than the average of all directions when the normalized backscatter radar cross section exceeds unity. In several theories, subsurface refractive structures with approximate spherical or hemispherical symmetry are invoked for this purpose, where an axis of symmetry results in markedly increased backscatter coherence relative to other directions. The peculiar polarization properties of the observed echoes, while not understood in detail, might well involve the decoupling of two characteristic electromagnetic modes, such as would occur during total internal reflections (Eshleman, 1986a, b). In this mechanism, the complex reflection coefficients for the two modes both have a magnitude of unity, but their phase differs and this constitutes an efficient method of decoupling. The observed bright-limb character of the scattering, plus the lack of an observable backscattered specular component, is explained in most of the theories by invoking volumetric

instead of surface scattering mechanisms. For example, Gurrola and Eshleman (1990) show a good match to the observed broad power spectra (and to the polarization and strength parameters) using a model with a uniform distribution of buried craters on the moons.

The principal requirement for progress in our understanding of electromagnetic interactions with icy outer-solar-system surfaces is obtaining data of a new type. This could be accomplished with the Galileo mission. Special emphasis should be placed on: (1) measuring the bi-static scattering as a function of time as the Galileo Orbiter passes between Earth and each of the three icy Galilean moons, as nearly as possible through the exact back scatter geometry; (2) measuring the specular and near-specular scattering from each of these surfaces for various geometries ranging up to the condition of near-grazing bi-static scattering; and (3) measuring scattering in the above geometries for different geological regions on the moons.

The first measurement would reveal the width and shape of the strong backscattered glory lobe, as well as its maximum strength. The width measurement would constitute a direct indication of a characteristic scale of the unknown scattering mechanism, such as the diameters of coherent scatterers or the mean path length of radar photons between subsurface scattering centers. The lobe shape and the polarization properties of the echoes near its peak could be diagnostic of significant properties of the surface and sub-surface material and could help guide theoretical modeling. For example, in one model the strongest scattering is in the form of a cone, with the exact backscatter direction being a local minimum on the axis of the cone, instead of being an isolated maximum. This local minimum, however, would be much stronger than the average scattering outside the conical region and would have different polarization properties. The second measurement would separate the 'usual' specular kinds of scattering from planetary surfaces from the strong backscatter glory produced by the icy moons, making possible an investigation into what is likely to be two fundamentally different kinds of interaction between electromagnetic waves and the near-surface material of these moons. The third proposed set of measurements would then provide the diagnostic results of the other two sets for characteristically different domains on the icy moons. Note that it is inherent that no radar investigation from Earth or from monostatic spacecraft systems could do the kinds of investigations described above, since they only measure the return at the exact center of the strong backscattered glory lobe.

The bi-static radar experiment would be based on dual-frequency downlink transmissions using the Galileo telecommunications system and the Earth tracking stations, although an investigation needs to be made of whether any useful information might also be obtainable from the uplink command links. The spacecraft high-gain antenna would need to be pointed and tracked for the required bi-static geometries. An investigation by R. A. Simpson of Stanford has been made of expected signal strengths for sample Galileo encounters with the outer Galilean moons. The results indicate that significant data could be obtained from the known strong scattering in and presumably near the back scatter geometry, and for the somewhat enhanced scattering that is expected for the oblique specular geometries (Simpson and Tyler, 1981). The detection of scattering, in other directions is problematical, but the geometries discussed above appear to be the key ones for help in discriminating among existing theories and for guidance in the construction of new theories.

Europa, Ganymede, and Callisto must have atmospheres, which may consist only of the extremely tenuous gas that would be due to vapor pressure equilibrium (VPE) of atmospheric water vapor with the cold surface ice. The constant interchange of water between atmospheres and surfaces in VPE might play a role in producing surfaces that display the strange scattering behaviors discussed above. In this regard, it now appears that there are just three solar-system bodies with substantial (surface pressure greater than one-millionth that of Earth) atmospheres where VPE with surface ices is the controlling factor (Eshleman *et al.*, 1990). These are Mars, Triton, and Pluto, where the main ice-vapor involved in the VPE control is CO<sub>2</sub> for Mars, N<sub>2</sub> at Triton, and CH<sub>4</sub> or possibly CO or N<sub>2</sub> on Pluto. (For Titan, VPE of N<sub>2</sub> with nitrogen in solution in surface hydrocarbon liquids may be involved (Lunine *et al.*, 1983).) Recall that the south polar cap of Mars produces at least some of the anomalous radar characteristics of the icy Galilean moons (Muhleman *et al.*, 1989).

It is clear that there are major puzzles attending the interaction of electromagnetic waves with the icy surfaces that occur in the outer solar system. An increase in understanding of this problem is needed both for applications and for basic knowledge about these surfaces. The Galileo mission has the potential of providing new insights based on a bi-static radar study of Europa, Ganymede, and Callisto, as experimental targets of opportunity.

### Acknowledgements

The authors gratefully acknowledge the assistance and support of the Galileo project staff at the Jet Propulsion Laboratory of the California Institute of Technology and at NASA Headquarters. Particular appreciation is due to members of the Radio Science Support team at JPL who represented the interests of the Radio Propagation team to the project from its inception in 1977 through launch in 1989 and are now conducting flight planning and operations. They are: Sami Asmar, Gerard Benenyhan, Jay Breidenthal, Joseph Brenkle, Susan Borutzki, Peter Doms, Paula Eshe, Daniel Finnerty, Carole Hamilton, Randy Herrera, Dwight Holmes, Tony Horton, Rob Kursinski, David Morabito, and Yong Ho Son.

This work is supported by NASA, BMFT, and the DLR.

\* Bundesministerium für Forschung und Technologie/Deutsche Forschungsanstalt für Luft- und Raumfahrt.

### References

Acuna, M. H. and Ness, N. F.: 1976, *J. Geophys. Res.* **81**, 2917.

Allison, M.: 1990, *Icarus* **83**, 282.

Anderson, J. D., Armstrong, J. W., Campbell, J. K., Estabrook, F. B., Krishner T. P., and Lau, E. L.: 1992, 'Gravitational Celestial Mechanics Investigations with Galileo', *Space Sci. Rev.* **60**, 591 (this issue).

Barnes, J. A., Chi, A. R., Cutler, L. S., Healey, D. J., Leeson, D. B., McGunigal, T. E., Mullen, J. A., Smith, W. L., Sydnor, R. L., Vessot, R. F. C., and Winkler, G. M. R.: 1971, *IEEE Trans. Instr. Meas.* **IM-20**, 105.

Bird, M. K.: 1982, *Space Sci. Rev.* **33**, 99.

Bird, M. K. and Edenhofer, P.: 1990, in R. Schwenn and E. Marsch (eds.), 'Remote Sensing Observations of the Solar Corona', *Physics of the Inner Heliosphere*, Springer-Verlag, Heidelberg.

Bird, M. K., Volland, H., Efimov, A. I., Stelzried, C. T., and Seidel, B. L.: 1985, paper presented at the 5th General Assembly of IAGA, Prague, Czechoslovakia, August 10.

Bird, M. K., Volland, H., Howard, R. A., Koomen, M. J., Michels, D. J., Sheeley, N. F., Jr., Armstrong, J. W., Seidel, B. L., Stelzried, C. T., and Woo, R.: 1985, *Solar Phys.* **98**, 341.

Campbell, D. B., Chandler, J. F., Ostro, S. J., Pettengill, G. H., and Shapiro, I. I.: 1978, *Icarus* **34**, 254.

Connerey, J. E. P.: 1987, *Rev. Geophys.* **25**, 615.

Connerney, J. E. P., Acuna, M. H., and Ness, N. F.: 1982, *J. Geophys. Res.* **86**, 3623.

Conrath, B. J., Gautier, D., Hanel, R. A., and Hornstein, J. S.: 1984, *Astrophys. J.* **282**, 807.

Conrath, B., Gautier, D., Hanel, R., Lindal, G., and Marten, A.: 1987, *J. Geophys. Res.* **92**, 15003.

Eshleman, V. R.: 1986a, *Nature* **319**, 755.

Eshleman, V. R.: 1986b, *Science* **234**, 587.

Eshleman, V. R.: 1987, *Adv. Space Sci.* **7**(5), 133.

Eshleman, V. R., Gurrola, E. M., Hinson, D. P., Lindal, G. F., Marouf, E. A., Simpson, R. A., and Tyler, G. L.: 1990, paper presented at the XXVIII COSPAR Conference, The Hague, 4 July.

Eshleman, V. R., Tyler, G. L., Anderson, J. D., Fjeldbo, G., Levy, G. S., Wood, G. E., and Croft, T. A.: 1977, *Space Sci. Rev.* **21**, 207.

Eshleman, V. R., Tyler, G. L., Wood, G. E., Lindal, G. F., Anderson, J. D., Levy, G. S., and Croft, T. A.: 1979a, *Science* **204**, 976.

Eshleman, V. R., Tyler, G. L., Wood, G. E., Lindal, G. F., Anderson, J. D., Levy, G. S., and Croft, T. A.: 1979b, *Science* **206**, 959.

- Fjeldbo, G., Kliore, A., Seidel, B., Sweetnam, D., and Cain, D.: 1975, *Astron. Astrophys.* **39**, 91.
- Fjeldbo, G., Kliore, A., Seidel, B., Sweetnam, D., and Woiceshyn, P.: 1976a, in T. Gehrels (ed.), 'The Pioneer 11 Radio Occultation Measurements of the Iovian Ionosphere', *Jupiter*, University of Arizona Press, Tucson, p. 238.
- Fjeldbo, G., Kliore, A., Sweetnam, D., Esposito, P., Seidel, B., and Howard, T.: 1976b, *Icarus* **29**, 439.
- Gierash, P. J. and Conrath, B. J.: 1985, *Recent Advances in Planetary Meteorology*, Cambridge University Press, Cambridge, p. 121.
- Goldstein, R. M. and Green, R. R.: 1980, *Science* **207**, 179.
- Goldstein, R. M. and Morris, G. A.: 1975, *Science* **188**, 1211.
- Gurrola, E. M. and Eshleman, V. R.: 1990, *Adv. Space Res.* **10**(1), 195.
- Hagfors, T., Gold, T., and Ierikic, H. M.: 1985, *Nature* **315**, 637.
- Hapke, B.: 1990, *Icarus* **88**, 407.
- Hinson, D. P.: 1984, *J. Geophys. Res.* **89**, 65.
- Hinson, D. P. and Magalhaes, J. A.: 1991, *Icarus*. in press.
- Hinson, D. P. and Tyler, G. L.: 1982, *J. Geophys. Res.* **87**, 5275.
- Hinson, D. P. and Tyler, G. L.: 1983, *Icarus* **54**, 337.
- Hollweg, J. V., Bird, M. K., Volland, H., Edenhofer, P., Stelzried, C. T., and Seidel, B. L.: 1982, *J. Geophys. Res.* **87**, 1.
- Horanyi, M., Cravens, T. E., and Waite, J. H.: 1988, *J. Geophys. Res.* **93**, 7251.
- Howard, H. T., Tyler, G. L., Esposito, P. B., Anderson, J. D., Reasenberg, R. D., Shapiro, I. I., Fjeldbo, G., Kliore, A. J., Levy, G. S., Brunn, D. L., Dickinson, R., Edelson, R. E., Martin, W. L., Postal, R. B., Seidel, B., Sesplaukis, T. T., Shirley, D. L., Stelzried, C. T., Sweetnam, D. N., Wood, G. E., and Zygielbaum, A. I.: 1974, *Science* **185**, 179.
- Ingersoll, A. P.: 1989, *Icarus* **81**, 298.
- Kliore, A. J., Fjeldbo, G., Seidel, B. L., Sweetnam, D. N., Sesplankis, T. T., Woiceshyn, P. M., and Rasool, S. I.: 1975, *Icarus* **24**, 407.
- Kumar, S.: 1985, *Icarus* **61**, 101.

Levy, G. S., Green, D. W., Royden, H. N., Wood, G. E., and Tyler, G. L.: 1981, *J. Geophys. Res.* **86**, 8467.

Lindal, G. F., Lyons, J. R., Sweetnam, D. N., Eshleman, V. R., Hinson, D. P., and Tyler, G. L.: 1987, *J. Geophys. Res.* **92**, 14987.

Lindal, G. F., Sweetnam, D. N., and Eshleman, V. R.: 1985, *Astron. J.* **90**, 1136.

Lindal, G. F., Wood, G. E., Levy, G. S., Anderson, J. D., Sweetnam, D. N., Hotz, H. B., Buckles, B. J., Holmes, D. P., Doms, P. E., Eshleman, V. R., Tyler, G. L., and Croft, T. A.: 1981, *J. Geophys. Res.* **86**, 8721.

Lunine, J. I., Stevenson, D. J., and Yung, Y. L.: 1983, *Science* **222**, 1229.

Muhleman, D. O., Butler, B. J., Grossman, A. W., Slade, M. A., and Jurgens, R.: 1989, paper presented at the Fourth International Mars Conference, Tucson, AZ, 10 January.

Muhleman, D. O., Grossman, A. W., Butler, B. J., and Slade, M. A.: 1990, *Science* **248**, 975.

Ostro, S. J.: 1982, in P. Morrison (ed.), *Satellites of Jupiter*, University Arizona Press, Tucson, p. 213.

Ostro, S. J. and Pettengill, G. H.: 1978, *Icarus* **34**, 268.

Ostro, S. J. and Shoemaker, E. M.: 1990, *Icarus* **85**, 335.

Ostro, S. J., Campbell, D. B., Pettengill, G. H., and Shapiro, I. I.: 1980, *Icarus* **44**, 431.

Pätzold, M., Bird, M. K., Volland, H., Levy, G. S., Seidel, B. L., and Stelzried, C. T.: 1987, *Solar Phys.* **109**, 91.

Pollack, J. B., Atkinson, D. H., Seiff, A., and Anderson, J. D.: 1992, *Space Sci. Rev.* **60**, 143 (this issue).

Simpson, R. A. and Tyler, G. L.: 1981, *Icarus* **46**, 361.

Tyler, G. L.: 1987, *Proc. IEEE* **75**, 1404.

Tyler, G. L., Sweetnam, D. N., Anderson, J. D., Borutzki, S. E., Campbell, J. K., Eshleman, V. R., Gresh, D. L., Gurrola, E. M., Hinson, D. P., Kawashima, N., Kursinski, E. R., Levy, G. S., Lindal, G. F., Lyons, J. R., Marouf, E. A., Rosen, P. A., Simpson, R. A., and Wood, G. E.: 1989, *Science* **246**, 1466.

Tyler, G. L., Vesecky, J. F., Plume, M. A., Howard, H. T., and Barnes, A.: 1981, *Astrophys. J.* **249**, 318.

- Volland, H., Bird, M. K., and Edenhofer, P.: 1983, in K.-P. Wenzel *et al.* (eds.), 'The ISPM Coronal Sounding . Experiment', *The International Solar Polar Mission - Its Scientific Investigations*. ESA SP-1050, p. 243.
- Volland, H., Bird, M. K., Levy, G. S., Stelzreid, C. T., and Seidel, B. L.: 1977, *J. Geophys. Res.* **42**, 659.
- Woo, R.: 1988, *J. Geophys. Res.* **90**, 154.
- Woo, R. and Armstrong, J. W.: 1979, *J. Geophys. Res.* **84**, 7288.
- Woo, R. and Armstrong, J. W.: 1981, *Nature* **292**, 608.
- Woo, R. and Ishimaru, A.: 1980, *Nature* **289**, 383.
- Woo, R. and Yang, F.: 1978, *J. Geophys. Res.* **83**, 5245.
- Woo, R., Armstrong, J. W., and Ishimaru, A.: 1980, *J. Geophys. Res.* **85**, 8031.
- Woo, R., Armstrong, J. W., and Kendall, W. B.: 1980, *Science* **205**, 87.
- Woo, R., Armstrong, J. W., Sheeley, N. R., Jr., Howard, R. A., Koomen, M. J., Michels, D. J., and Schwenn, R.: 1985, *J. Geophys. Res.* **90**, 154.
- Woo, R., Armstrong, J. W., Sheeley, N. R., Jr., Howard, R. A., Michels, D. J., and Koomen, M. J.: 1982, *Nature* **300**, 157.
- Yeh, K. C. and Liu, C. H.: 1972, *Theory of Ionospheric Waves*, Academic Press, New York.